

Acoustic Wavefront Manipulation: Impedance Inhomogeneity and Extraordinary Reflection

Jiajun Zhao^{1,2}, Cheng-Wei Qiu¹, Zhining Chen¹, and Baowen Li^{2,3}

¹*Department of Electrical and Computer Engineering,*

National University of Singapore, Singapore 117576, Republic of Singapore

²*Department of Physics and Centre for Computational Science and Engineering,*
National University of Singapore, Singapore 117546, Republic of Singapore and

³*NUS-Tongji Center for Phononics and Thermal Energy Science,*

School of Physical Science and Engineering, Tongji University, Shanghai 200092, People's Republic of China

(Dated: December 31, 2021)

Optical wavefront can be manipulated by interfering elementary beams with phase inhomogeneity. Therefore a surface allowing huge, abrupt and position-variant phase change would enable all possibilities of wavefront engineering. However, one may not have the luxury of efficient abrupt-phase-changing materials in acoustics. This motivates us to establish a counterpart mechanism for acoustics, in order to empower the wide spectrum of novel acoustic applications. Remarkably, the proposed impedance-governed generalized Snell's law (IGSL) of reflection is distinguished from that in optics. Via the manipulation of inhomogeneous acoustic impedance, extraordinary reflection can be tailored for unprecedented wavefront manipulation while ordinary reflection can be surprisingly switched on or off. Our results may power the acoustic-wave manipulation and engineering. We demonstrate novel acoustic applications by planar surfaces designed with IGSL.

Refraction, a physical phenomena in classic optics, was recently re-visited from the viewpoints of complex refractive index of a bulky medium[1], abrupt phase change of an interface [2], and diffraction theory for gratings [3]. These works also shed light on the relation between the reflection and incidence, interpreted as the generalized Snell's law of reflection (GSL) [2], which plays a novel role on optical wavefront engineering and has resulted in promising accomplishments [4–8]. The phase inhomogeneity, functioning as the underlying principle of optical GSL, metamorphoses the original (ordinary) reflection into the anomalous reflection through abrupt phase changes obtained at different positions of the interface made of thin metallic nanoantenna array. Fundamental physics may be explained by phase antenna array [9–11].

GSL is based on Fermat's principle and hence the law should hold for various wave types: electromagnetic and acoustic waves. But one cannot analogously translate the GSL from electromagnetics to acoustics, since the naturally available materials which can give the abrupt phase change to the wave are limited in acoustics. Hence, the luxury of using metallic meta-surface [2, 4] to fulfill the phase control is no more available, and it is necessary to establish a distinct principle to manipulate the acoustic waves. Our findings also reveal acoustic GSL is more complicated than that for electromagnetics. In addition, the polarization of the anomalous reflection controlled by electromagnetic GSL discords with that of the incidence, though this is not explicitly presented in the law of electromagnetic GSL [2].

In this Letter, we establish the framework of acoustic wavefront manipulation by resorting to specific acoustic impedance (SAI) [12] inhomogeneity, rather than the phase control as Refs. [1, 2] in optical regime. More specifically, the inhomogeneous SAI will generally give rise to one ordinary reflection (analogous to anomalous

reflection in [2] controlled by GSL) and one extraordinary reflection (uniquely pronounced in impedance-governed generalized Snell's law of reflection in acoustics, i.e., IGSL).

In optical GSL [2], the so-called anomalous reflection actually corresponds to the situation when the original ordinary reflection is deflected toward a “wrong” direction governed by GSL. On the contrary, the ordinary reflection in IGSL cannot be altered by an acoustic SAI interface, but IGSL can provide insight to the design of SAI interface so as to “turn off” the ordinary reflection. Moreover, the extraordinary reflection governed by IGSL is an additionally unique component in acoustic cases, which can be “geared” along arbitrary directions in principle with vanishing ordinary reflection simultaneously. Therefore our proposed IGSL can lead to richer effects and applications in acoustics.

The impedance Z_n of the flat SAI surface is expressed in a complex form $Ae^{-i\psi(y)}$, where A is the amplitude and $\psi(y)$ is the phase angle along the surface. Since the SAI is inhomogeneous, both the real and the imaginary parts of Z_n change spatially. The intensity of an acoustic wave depends on the real part of a SAI and the root-mean-square acoustic velocity \mathbf{v}_{rms} , i.e., $I = \text{Re}(Z_n)v_{rms}^2$. Therefore, it is reasonable to set the real part of the SAI as a constant so that only one variable determines the intensity. In this connection, one may consider $Z_n = Ae^{-i\psi(y)}/\cos\psi(y)$, since A is an arbitrary value. Now the real constant A in the new form of Z_n corresponds to the constant resistance of the SAI. After some algebraic treatment in the phase angle for the convenience of derivation, we thus obtain

$$Z_n(y, \omega) = A \frac{1}{\cos[\psi(y)/2]} e^{-i\psi(y)/2}, \quad (1)$$

in which case both the ordinary and extraordinary re-

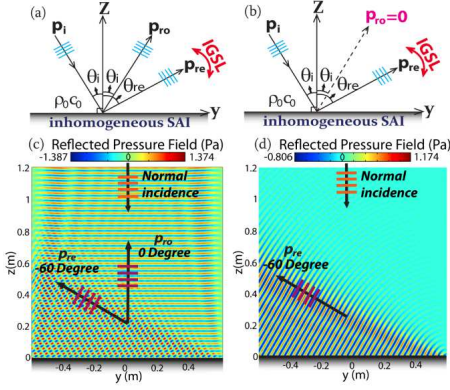


FIG. 1. Schematic of IGSL. p_i , p_{ro} , and p_{re} denote the incident acoustic wave, ordinary reflection, and the extraordinary reflection. θ_i is the incident angle of p_i . (a) For a flat interface with an inhomogeneous SAI, the angle of p_{ro} , i.e., θ_{ro} , is not influenced, while p_{re} occurs simultaneously and the angle θ_{re} is controlled by IGSL. (b) If SAI is properly controlled, p_{ro} can be nulled. Ultrasound with unit amplitude and $\omega = 300Krad/s$ is normally impinged upon SAI surfaces from water. (c) The SAI along the flat surface $z = 0$ leads to both p_{ro} and p_{re} when an arbitrary A is chosen in Eq.(1). (d) A particular SAI inhomogeneity is chosen according to Eq.(6). $\psi(y) = -100\sqrt{3}y$ is selected throughout.

reflections exist for a general A . Note that ω -dependency on the right hand side of Eq.(1) is included into $\psi(y)$. According to our derivation provided in Supplement Materials (Section I), the directivity factor governing the extraordinary reflection is

$$\Psi(\theta_{re}, \omega) = \int_{-\infty}^{\infty} \frac{\rho_0 c_0}{2A} e^{i\psi(y)} e^{i\frac{\omega}{c_0}(\sin\theta_i - \sin\theta_{re})y} dy, \quad (2)$$

where ρ_0 and c_0 represent the density of the ambient medium and the speed of sound in the upper space in Fig. 1. The integration of Eq. (2) consequently results in a Dirac delta function

$$\Psi(\theta_{re}, \omega) = \frac{\rho_0 c_0}{2A} \delta[k_0 y(\sin\theta_i - \sin\theta_{re}) + \psi(y)], \quad (3)$$

which makes sense only for $k_0 y(\sin\theta_{re} - \sin\theta_i) = \psi(y)$. $k_0 = \omega/c_0$ stands for the wave number. Hence the relation between the incident angle and the angle of extraordinary reflection satisfies:

$$k_0[\sin\theta_{re} - \sin\theta_i] = d\psi(y)/dy. \quad (4)$$

Although IGSL's form seems similar to GSL, its physical origin and the meaning of $\psi(y)$ are dramatically different from those of optical GSL [1, 2, 4]. Moreover, IGSL only serves to redirect the extraordinary reflected wave arbitrarily, with no influence on the direction of ordinary reflection. In the mean time, Eq. (4) sheds a light to an extreme angle (similar to critical angle):

$$\theta_e = \begin{cases} \arcsin(-1 - \frac{1}{k_0} \frac{d\psi(y)}{dy}), & \text{if } \frac{d\psi(y)}{dy} < 0 \\ \arcsin(+1 - \frac{1}{k_0} \frac{d\psi(y)}{dy}), & \text{if } \frac{d\psi(y)}{dy} > 0 \end{cases}, \quad (5)$$

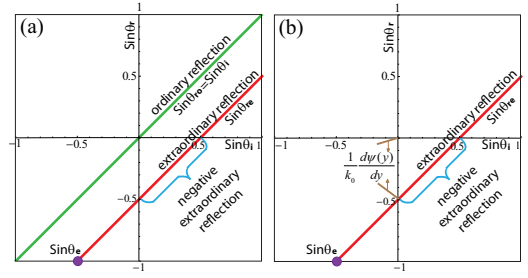


FIG. 2. Reflection angles $\sin\theta_{ro, re}$ versus $\sin\theta_i$ when $k_0 = 10rad/m$ and $\psi(y) = -5y$. Ordinary (green line) and extraordinary reflections (red line) emerge simultaneously in (a). In (b), only extraordinary component is present for the same parameters of (a) except A . The purple dot denotes $\sin\theta_e$ in Eq. (5).

above which extraordinary reflection becomes evanescent. Equation (5) holds only if $-1 \leq 1 - \frac{1}{k_0} \left| \frac{d\psi(y)}{dy} \right| \leq 1$. Otherwise, extraordinary reflection does not propagate in the upper space.

Usually, both p_{ro} and p_{re} will coexist as shown in Fig. 1(a), suggesting *double* reflection, while IGSL only controls the angle of extraordinary reflection θ_{re} . Hence, it is interesting to eliminate p_{ro} in Fig. 1(b), by means of a particularly selected value of A in Eq. (1). Our elaboration in Supplement Materials (Section I) suggests that $A = (\rho_0 c_0)/(2 \cos\theta_i)$ can make p_{ro} vanished, i.e., the ordinary reflection is switched off, as shown in Fig. 1(b,d). Corresponding SAI of the flat surface is

$$Z_n(y, \omega) = \frac{\rho_0 c_0}{2 \cos\theta_i} \frac{1}{\cos[\psi(y)/2]} e^{-i\psi(y)/2}. \quad (6)$$

Only at such condition, acoustic IGSL behaves as an exact counterpart of optical GSL whereas the mechanisms are completely different.

Supposing the gradient of $\psi(y)$ along the flat interface in Eq. (6) is constant, it can be predicted from Eq.(4) that the wavefront of extraordinary reflection will propagate as a plane acoustic wave, independent of the location y . We selected water ($\rho_0 = 1kg/m^3$; $c_0 = 1500m/s$ [12]) in the upper space, $\omega = 300Krad/s$ as the circular frequency, $e^{-ik_0 z}$ as the normal incident plane ultrasound, and a linear form of $\psi(y) = -100\sqrt{3}y$ in Eq. (6).

The angle of extraordinary reflection is theoretically found to be -60° by IGSL, validated by our simulation in Fig. 1(d). The ordinary one is thoroughly suppressed thanks to the specific A chosen according to Eq.(1). The vanished ordinary reflection is achieved by adjusting the SAI so as to make the incident angle meets the angle of intromission [12]. In contrast, in Fig. 1(c), the same parameters are kept except for another option for A , whose value is arbitrarily taken to be $2\rho_0 c_0$. It clearly shows that the ordinary reflection occurs, and meanwhile the extraordinary one still keeps the same angle -60° , verifying the stability of our theoretical formulation.

Figure 1(d) has suggested the possibility of negative extraordinary reflection, which is verified for oblique in-

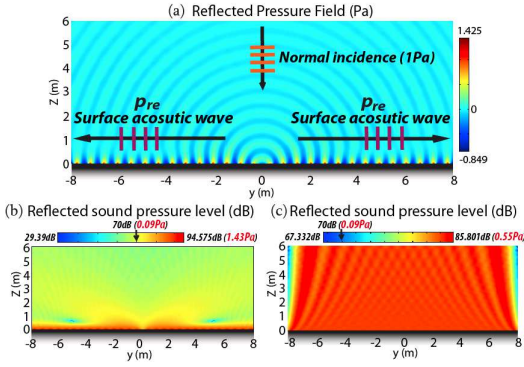


FIG. 3. Conversion of PAWs to SAWs via SAI interface. The PAW with unit amplitude and $\omega = 15Krad/s$ is normally incident from water. Only reflected acoustic pressure is plotted. (a) The SAI of Eq.(6) is set to be $\psi(y) = -11y$ for $y < 0$ and $\psi(y) = 11y$ for $y > 0$. SAWs are bifurcated at the origin and confined near the surface when propagating. (b) The reflected sound pressure level of (a). (c) The reflected sound pressure level when a homogeneous SAI as in Eq.(6) with $\psi(y) = 11$ is adopted instead.

idence in Fig. 2. In Fig. 2(a), because of the inhomogeneous SAI and the arbitrary A in Eq. (1), both ordinary reflection and extraordinary reflections occur. Fig. 2(b) depicts the same situation except for the ordinary reflection being switched-off as a result of the specifically chosen A according to Eq. (6), while the red line stays put as that in Fig. 2(a). The blue braces along the red line (extraordinary reflection) represent the region of negative reflection. It is noteworthy that extraordinary reflection does not exist if an incident angle is beyond the extreme angle $\theta_e = -30^\circ$ as described in Eq. (5), corresponding to the purple dots in Fig. 2.

To demonstrate IGSL's capability of designing novel acoustic devices, we proposed a SAI surface which can convert a propagating acoustic wave (PAW) to a surface acoustic wave (SAW) in Fig. 3. It can be verified from IGSL that the extreme angle 0° in Eq.(5) demands $\psi(y) = \pm 10y$. Therefore, one can set the SAI of Eq. (6) slightly beyond that extreme, e.g., $\psi(y) = -11y$ for $y < 0$ and $\psi(y) = 11y$ for $y > 0$ is set along the flat interface and symmetric with respect to the z axis. In Fig. 3(a), the arrows with purple crossbars label the paths of the bidirectional surface acoustic waves, which are caused by the evanescent extraordinary reflection owing to the inhomogeneous SAI interface, with a bit diffraction implicating the ideally perfect conversion. In contrast, if one uses an inappropriate SAI as in Eq.(6) with $\psi(y) = 11$ along the flat surface (the homogenous SAI does not generate extraordinary reflection; only ordinary reflection occurs), the reflected sound pressure level in Fig. 3(c) is almost uniformly spread over the space.

Figure 3(b) clearly demonstrates that the acoustic field is well confined in the region close to the interface and attenuated quickly to around $0Pa$ away from the interface, revealing the nearly perfect conversion. Interestingly, it shows in [13] that the meta-surface (H-shaped design)

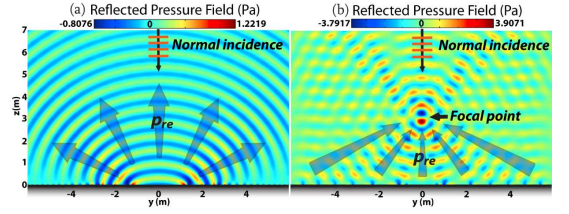


FIG. 4. Wavefront metamorphosis via SAI interface. A plane acoustic wave of $\omega = 15Krad/s$ is normally incident from water. Only reflected acoustic pressure is plotted. (a) The SAI of Eq.(6) with $\psi(y) = 2.5y^2$ is set along the flat surface. Extraordinary reflection, represented with the translucent arrows, diverges in a different wavefront. (b) The SAI of Eq.(6) with $\psi(y) = -10(\sqrt{y^2 + 3^2} - 3)$ is set. Extraordinary reflection converges to a focal point in the two-dimensional case.

provides an extra momentum to overcome the momentum mismatch from a propagating electromagnetic wave to a surface one, in which a mushroom structure in addition to the fractal surface played a dispensable role to continuously couple out the surface electromagnetic wave generated by the fractal. This prevents the propagating electromagnetic waves from being reflected back to the upper space. Hence, our PAW-SAW conversion in acoustics, originating form a distinguished mechanism, is differentiated from [13] in terms of physical principle and application domain.

From Fig. 3, one may notice that such technology can function as an alternative invisibility acoustic cloak by trapping the acoustic field in the vicinity of the coating, resulting in much lower signal strength of the reflection. It may pave the avenue to the large size acoustic invisibility since it is only dependent on the surface technique instead of wave-interaction based metamaterial acoustic cloaking [14].

If one considers the PAW-SAW conversion to be a creation of acoustic cognitive deception, our IGSL can also metamorphose acoustic pressure fields everywhere through SAI manipulation. This deception effect is obtained by manipulating plane wavefronts into wavefronts generated by a virtual source or focusing illumination, governed by the control of extraordinary reflection by means of IGSL. Under these scenarios, we need to consider nonlinear form of $\psi(y)$, which means the right hand side of Eq.(4) relies on y . New phenomena can thus be expected when the angle of extraordinary reflection becomes spatially varying.

It is found that the acoustic deception can indeed be created by IGSL, e.g., a quadratic SAI $\psi(y) = 2.5y^2$ in Eq. (6) resulting in ordinary reflection eliminated. Correspondingly, the angle of extraordinary reflection in Fig. 4(a) is a position-dependent function $\sin \theta_{re} = 0.5y$, functioning only within the region of $-2 \leq y \leq 2$ of the SAI interface. Within this particular region, the extraordinary reflected waves will fan out into the upper space as demonstrated in Fig. 4(a), which verifies our theoretical prediction. Beyond $-2 \leq y \leq 2$, no propagating

extraordinary reflection can be excited owing to Eq.(5). Therefore, IGSL can be employed to camouflage a flat surface as if there were an emitting source at the origin instead of the physical planar interface. The dual effect by camouflaging curvilinear interfaces by a virtually flat one, by manipulating the convex wavefronts into planar wavefronts, was reported in plasmonic regime [15].

Furthermore, the SAI can be manipulated to let acoustic waves reflected by a planar interface be focused as well. In optics, a flat lens with metallic nanoantennas of varying sizes and shapes can consequently converge the transmitted light to a focal point [5, 6]. It is worth noting that the optical focal controlled by optical generalized Snell's law of refraction is on the other side of incoming light, i.e., on two sides of the flat surface [5, 6] in the transmission mode. On the contrary, in acoustics, we employed an inhomogeneous SAI flat surface to focus the extraordinary reflection wave, in the reflection mode suggested by IGSL developed in this Letter.

This *ipsilateral* focusing, as demonstrated in Fig. 4(b), is thus obtained in the planar geometry in acoustics for the first time. In Eq. (6), a hyperbolic form was set $\psi(y) = -k_0(\sqrt{y^2 + f^2} - f)$ (f being the given focal length [16]) for the SAI of the flat interface. Extraordinary reflections from different angles constructively interfere at the ipsilateral focal point, as if the waves are emerging from a parabolic surface. The parameters in Fig. 4(b) are the same as those in Fig. 4(a) except for the specific hyperbolic SAI form $\psi(y) = -10(\sqrt{y^2 + 3^2} - 3)$, with the designed focal point at $(y = 0, z = 3)$ and the ordinary reflection suppressed. In addition, the simulated acoustic pressure at the focal point is well confined at $(y = 0, z = 3)$.

Interestingly, the imaging on the same side was only possibly presented in [17] for electromagnetic waves, which demands strong chiral materials filled in the whole upper space and the propagating wave excited inside the filling chiral material. The same-side imaging is only a partial imaging, i.e., only one circularly polarized wave being imaged and the other circularly polarized wave being reflected ordinarily. In addition, it is usually challenging to get high chirality. In acoustics, we do not have the luxury of finding strong chiral materials and our ipsilateral imaging is achieved by translating all the stringent

requirements of the half-space chiral materials into an inhomogeneous impedance surface, and this phenomenon is independent of circular polarization status.

Although we have shown robust capabilities of IGSL in obtaining novel acoustic applications, it is still far from the theoretical boundaries of what IGSL can be used to achieve. Nevertheless, an equally important thing is to provide feasible schemes to realize SAI by acoustic elements. In this connection, one representative example is suggested for Eq. (1). Expanding Eq. (1) leads to $A - iA \tan[\psi(y)/2]$. In order to enhance the reflection and reduce the absorption, it is imperative to have much larger imaginary part than the real part, i.e., $\tan[\psi(y)/2]$ being so large that the real part of SAI can be ignored.

One method to realize the large $-iA \tan[\psi(y)/2]$ can be approached by using hard-wall tubes with a pressure-release termination [12], i.e., $-i\rho_t c_t \tan(\omega d/c_t)$ where ρ_t and c_t are the density and the sound speed of the medium in the tube respectively, and d denotes the length of the tube. The linear change of d will result in the linear change of $\psi(y)/2$ correspondingly. If the range of d leads to large $\tan[\psi(y)/2]$ and the tubes with linearly increasing lengths are juxtaposed perpendicular to one surface, particular SAI inhomogeneity can be realized approximately by impedance discontinuity.

To conclude, the impedance-governed generalized Snell's law of reflection was established for novel manipulations of acoustic wavefronts. It is inspired by GSL which exploits abrupt-phase-changing materials in optics, but the fundamental principle of IGSL completely differs from that of GSL. IGSL can turn off ordinary reflection and control extraordinary reflection in acoustics. GSL is only analogous to such special situation of IGSL. We not only theoretically demonstrated interesting manipulations of acoustic wave but also provided insightful realization schemes for engineers. In addition, the cross polarization is not present in acoustics. As a few examples, we demonstrated acoustic PAW-SAW conversion, acoustic disguise, acoustic planar lens, and acoustic ipsilateral imaging. These novel acoustic effects will inspire new technologies and devices on acoustic wave engineering and manipulation, leading to unprecedented applications.

We thank Prof. Andrea Fratallocchi and Prof. Nanfang Yu for stimulating discussion and advices.

-
- [1] B. Sundar, A. C. Hamilton and J. Courtial, *Opt. Lett.* **34**, 374 (2009).
 [2] N. Yu, P. Genevet, M. A. Kats, F. Aieta, J. P. Tetienne, F. Capasso and Z. Gaburro, *Science* **334**, 333 (2011).
 [3] S. Larouche and D. R. Smith, *Opt. Lett.* **37**, 2391 (2012).
 [4] X. Ni, N. K. Emani, A. V. Kildishev, A. Boltasseva and V. M. Shalaev, *Science* **335**, 427 (2012).
 [5] M. Kang, T. Feng, H. T. Wang, J. Li, *Opt. Express* **20**, 15882 (2012).
 [6] F. Aieta, P. Genevet, M. A. Kats, N. Yu, R. Blanchard, Z. Gaburro and F. Capasso, *Nano Lett.* **12**, 4932 (2012).
 [7] L. Huang, X. Chen, H. Muhlenbernd, G. Li, B. Bai, Q. Tan, G. Jin, T. Zentgraf and S. Zhang, *Nano Lett.* **12**, 5750 (2012).
 [8] P. Genevet, N. Yu, F. Aieta, J. Lin, M. A. Kats, R. Blanchard, M. O. Scully, Z. Gaburro and F. Capasso, *Appl. Phys. Lett.* **100**, 013101 (2012).
 [9] N. Engheta, *Science* **334**, 317 (2011).
 [10] C. A. Balanis, *Antenna Theory: Analysis and Design, 3rd edition* (Wiley, 2005), p. 300.

- [11] Z. N. Chen, in *Antennas for Portable Devices*, edited by Z. N. Chen (Wiley, 2007).
- [12] D. T. Blackstock, *Fundamentals of physical acoustics* (Wiley, 2000), p. 46, 136, 193, 512.
- [13] S. Sun, Q. He, S. Xiao, Q. Xu, X. Li and L. Zhou, *Nat. Mater.* **11**, 426 (2012).
- [14] S. Zhang, C. Xia and N. Fang, *Phys. Rev. Lett.* **106**, 024301 (2011).
- [15] J. Renger, M. Kadic, G. Dupont, S. S. Acimovic, S. Guenneau, R. Quidant and S. Enoch, *Opt. Express* **18**, 15757 (2010).
- [16] E. Hecht, *Optics, 3rd edition* (Addison Wesley, 1997).
- [17] C. Zhang and T. J. Cui, *Appl. Phys. Lett.* **91**, 194101 (2007).